INCREASING THE JOINT STRENGTH OF ULTRASONIC-SPOT WELDED FIBER-REINFORCED LAMINATES BY AN INNOVATIVE PROCESS CONTROL METHOD

Shahan Tutunjian[1,2], Oğuzhan Eroğlu[1], Martin Dannemann[2], Niels Modler[2] & Fabian Fischer[1]

[1]Joining Technologies, Welding Process & Bolting, BMW Group, Munich Germany
Email: Shahan.Tutunjian@bmw.de, Web Page: https://www.bmwgroup.com
Email: Oguzhan.Eroglu@bmw.de, Web Page: https://www.bmwgroup.com
Email: Fabian.Fischer@bmw.de, Web Page: https://www.bmwgroup.com
[2] Institute of Lightweight Engineering and Polymer Technology, Technische Universität Dresden, Dresden Germany
Email: Martin.Dannemann@tu-dresden.de, Web Page: http://tu-dresden.de/mw/ilk
Email: Niels.Modler@tu-dresden.de, Web Page: http://tu-dresden.de/mw/ilk

Keywords: Ultrasonic welding, thermoplastic composites, spot welding, control system.

Abstract
The ultrasonic welding of carbon fiber-reinforced thermoplastic laminates received a wide interest from researchers in many fields, mainly in the aerospace and automotive industries. It allows the efficient joining of fiber-reinforced thermoplastic structural parts through the spot welding approach with a high level of automation. In this paper the differential ultrasonic spot welding method is briefly illustrated and a logical control system for this welding process is investigated. One of the main challenges of the differential ultrasonic welding is the overheating of the weld spot. To overcome this critical problem an active weld control method is suggested and investigated. The new method is based on the observation of the phenomena that the consumed power by the welder is in correlation with the temperature in the weld spot. It is assumed that if the power time derivative exceeds a certain value, then the ultrasonic displacement amplitude should be reduced by the controller. Consequently, the temperature in the weld spot can be indirectly regulated and a weld spot temperature in an acceptable range may be realized. The effectiveness of the control system is analyzed by means of weld temperature measurements and mechanical strength tests.

1. Introduction

The application of fiber-reinforced thermoplastics in the car body as both structural and add-on parts offers a wide range of advantages, such as high specific strength, high corrosion resistance and increased efficiency. In addition to the excellent material properties, these composites allow the utilization of efficient processing techniques such as thermoforming and fusion bonding [1]. These properties in turn allow the cost-effective production of modern lightweight vehicles that offer higher performance and comfort with lower energy consumption. One remarkable joining method for these composites is the ultrasonic welding [2]. Mechanical vibrations with a frequency above the audible spectrum (between *20 kHz* and *45 kHz*) are applied through a metallic horn perpendicular on the work-piece accompanied with a static pressure. The vibrations cause intensive intermolecular and boundary friction heating at the joint interface which in turn heats up locally until a sufficient temperature is reached and the polymers diffuse [3]. The conventional ultrasonic welding techniques for joining thin walled thermoplastic composites require the presence of energy directors in the weld interface at the required weld location. Such an approach is intensively investigated by Benatar et al. [4–6]. They concluded in their work that a good bond quality is achieved when the melt fronts of the adjacent energy directors meet and this event can be traced by the quick rise in the welder power. Villegas et al. [7–9] investigated an ultrasonic welding approach, in which a thin neat matrix film is placed separately in the weld interface as a flat energy director. In this method the researchers monitored the process through displacement and power curves. David Grewell [10] reported in his research

on the ultrasonic welding of neat thermoplastic parts that the efficiency of the ultrasonic welding process can be increased by using a pre-defined weld force and amplitude profile.

In this paper a new welding method is briefly introduced which eliminates the need for the energy directors. However, one of the main challenges of this method is the overheating and consequently the decomposition of the matrix at the weld spot. To overcome this drawback a logical weld-process control method is presented and its influence on the weld strength improvement is investigated.

2. The Differential Ultrasonic Spot Welding Method

The differential ultrasonic spot welding (DUS) is developed in the frame of this research work. It enables the welding of thin-walled thermoplastic composite laminates without the need for any sort of energy directors in the contact interface at the weld spot. The focusing of the vibration energy at the weld spot is done through the cyclic deformation shape of the laminates.

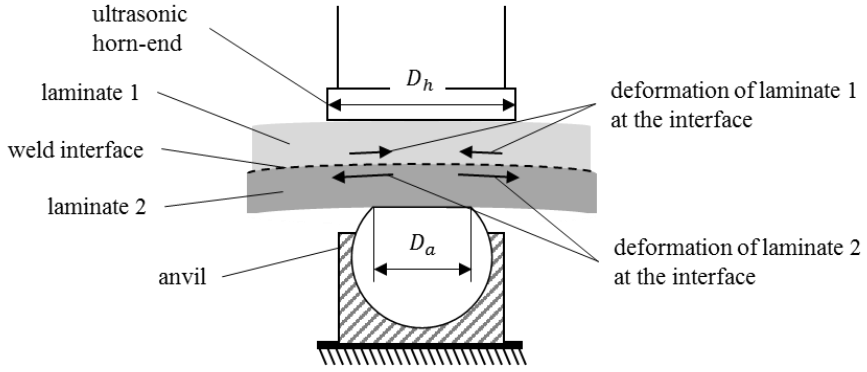

Figure 1. Schematic illustration of the laminate deformation shape at the compression phase of the ultrasonic cycle during the DUS-welding.

The welding takes place between an ultrasonic horn and an anvil. The contact diameter of the horn D_h is larger than the contact diameter of the anvil D_a. Due to the difference between these diameters and under the applied cyclic displacement the laminates compress and bend simultaneously. Consequently, the contacting surfaces at the weld interface deform in opposite directions and to different extents. As a result a friction relative movement takes place at the weld interface. This phenomena is illustrated schematically in Fig. 1. The amount of the heat flux density generated by the friction in the weld interface is given based on [8] by the following equation (Eq. 1):

$$\dot{q}_{fric}(T) = \alpha f \mu(T) u_0 \sigma_0 \, . \tag{1}$$

Even though the interfacial slippage amplitude u_0 is small, but at a high frequency f*=30 kHz* and under an adequate interfacial pressure σ_0 an intensive friction heat flux is generated. The friction causes the matrix to melt only locally at the interface. As soon as the matrix melts, almost the entire strain energy focuses at those molten layers. After this event the friction heating is eliminated and the viscoelastic volumetric heat generation dominates. The amount of viscoelastic heat per unit time per unit volume $\dot{q}_{visc}(T)$ can be expressed by the following equation (Eq. 2) where α is the hammering effect coefficient, $E``(T)$ is the temperature dependent loss modulus and ε_0 is the cyclic strain amplitude [8]:

$$\dot{q}_{visc}(T) = 0.5\alpha^2\pi f E``(T)\varepsilon_0^2 \,. \quad (2)$$

In the DUS welding the focused strain in the molten layers gets extremely high that if the weld is not properly controlled, the temperature continues to rise very rapidly to relative high temperatures until the matrix gradually decomposes. The decomposition of the matrix causes defects in the weld spot in the form of cavities, delamination and gas entrapments which in turn reduce the strength of the weld spot.

3. Experimental Setup

3.1. The Control System and Instruments

The power *P* consumed by the welder during the DUS is found to be proportional to the average temperature and to the temperature gradient in the weld spot. Therefore, it is assumed that if the power output of the welder is controlled it may be possible to indirectly control the weld temperature and consequently retain it in an acceptable range for an adequate duration of time.

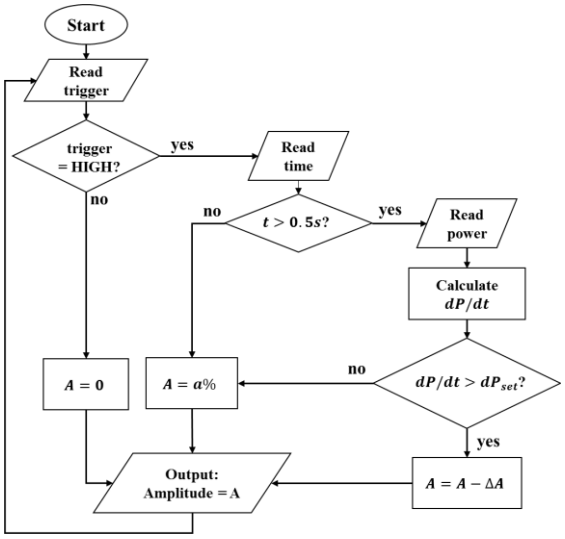

Figure 2. The algorithm of the DUS weld logical control system.

The algorithm for the controller is illustrated in Fig. 2. The controller calculates in real-time the derivative of the measured power dP/dt and checks with a constant sample rate within an if-loop for a certain condition of the derivative dP_{set} to be exceeded. If the dP/dt exceeds the dP_{set} then the controller gives the command to the welder to reduce the pre-set amplitude *A* with a step-value of ΔA. The drop in the amplitude occurs step-wise for each internal loop of the controller until the dP/dt becomes less than the dP_{set}. With this approach it is ensured that the weld power and consequently the weld temperature do not undergo a sudden increase as soon as the matrix gets melted. A time delay t_d*=0.5 s* is applied before the activation of the controller to avoid the early reduction of the amplitude at the weld initiation phase.

The ultrasonic welder is capable of outputting a nominal maximum power of *2400 W* with a nominal mean frequency of *30 kHz*. The ultrasonic stack consists of a *30 kHz* converter, a *2:1* titanium booster and a *4:1* catenoidal flat-end steel horn. The horn-end has a diameter of D_h*=18 mm* and the anvil has a diameter of

D_a*=10 mm*. The anvil is constructed in a way that it has a natural frequency of about *42 kHz* to avoid resonance vibrations within the rig. According to laser vibrometer measurements, this stack provides a maximum base-to-peak displacement amplitude $A_{100\%}=2.8x10^{-2}$ *mm* at the horn-end. The amplitude of the welder can be adjusted in terms of percentage from the maximum available amplitude. During welding it can be varied through an external analog signal input to the ultrasonic generator. *10 V* analog signal from the controller sent to the generator corresponds to *A=0%* amplitude and *0 V* corresponds to *A=100%.*

3.2. Mechanical Testing and Weld Configuration

The cross-tension test method is adopted to study the strength improvement of the controlled weld spot over its uncontrolled counterpart. In this method the plates (or laminates) are positioned as illustrated in Fig.3-(left) and the spot weld is located on their coinciding center of symmetries. The cross-tension test is carried out by fixing the welded plates at their ends (at the part laying outside the overlapping area) by using the fixing tool shown in Fig. 3-(right). The laminate ends are pressed between the two faces of the fixing jaws and the tension force is applied through the connecting ends of the tool with a rate of *2 mm/min*. The force at the weld spot break is considered for the comparative analysis and eventually it is used to calculate the weld strength by dividing it through the resulting weld spot break-surface area.

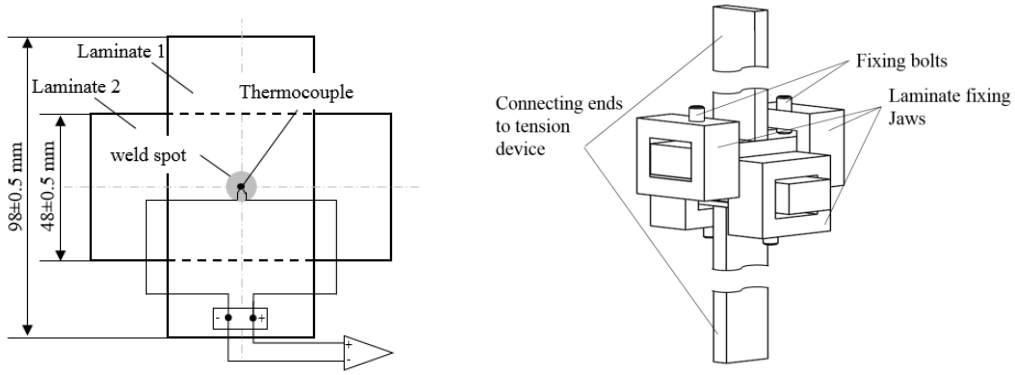

Figure 3. Cross-tension test specimen (left) and the corresponding clamping tool (right).

3.3. Specimen

The specimens used for the experimental studies are cut from 12K 2x2-twill carbon woven fabric-reinforced thermoplastic laminates. The matrix is a high fluidity Polyamide 6.6 (Nylon 6.6) with a glass transition at T_g*=69°C*, the melt onset temperature is at *243 °C*, the melt point T_m*=260 °C*, and the thermal decomposition temperature is *400°C*. The laminates are consolidated with the hot plate press approach. The final thickness of $h = 2.1 \pm 0.05$ mm is resulted by stacking the prepregs in the cross-ply sequence with a nominal fiber volume fraction of V_f*=50%.* The specimens are dried in an oven at *75 °C* for a minimum duration of *96 h* before welding to ensure that the laminates are free from excessive water content.

For the temperature measurement experiments the thermocouples are prepared by twisting and arc welding the ends of a fine gauge *40* (*0.08 mm*) K-type thermocouple wire pair. The thermocouples are carefully placed in the center of the laminate pairs and incorporated into the matrix by applying a short pulse (*0.2 s*) of ultrasonic vibration with an adequate static force on it.

3.4. Experiment plan

The experiments are divided into two groups. In the first, the laminates are welded without the weld control and under a constant vibration amplitude at *A=80% (2.2x10^{-2} mm)*. In the uncontrolled cases the influence of the weld duration (t_w) is investigated for three levels: UC-1 at t_{w1}*=1.8 s*, UC-2 at t_{w2}*=2.5 s* and UC-3 at t_{w3}*=3 s*. In the second group, the welds are controlled and the weld duration is set constant at t_{wc}*=2.5 s* and the weld control criteria is varied. One may understand under the weld control criteria, the value of the power time derivative dP_{set} at which the amplitude drop is triggered. The investigated cases are as follows: C-1 at dP_{set1}*=100 W/s*, C-2 at dP_{set2}*=200 W/s* and the C-3 at dP_{set3}*=300 W/s*. The initial amplitude value is set at *A=80%* and the amplitude drop value at each loop is set constant at *ΔA=1%* (*2.8x10^{-4} mm*). The most relevant process variables which are set constant are: the weld static force (*700N*), the static force at the solidification phase (*500N*) and the solidification time (*2 s*). In both of the test groups, several repetitions for each test set were done to gather statistical data.

4. Results and Discussions

4.1. The Analysis of the Power and the Temperature Curves

The temperature and power curves for the uncontrolled weld case UC-2 are plotted in Fig. 4. The dashed line represents the time trace of the temperature measured in the spot weld for one of the repetitions and the solid line refers to the corresponding consumed weld power. The shaded blue and grey areas around the curves are the ranges covered by the time traces of the temperature and the power respectively for the remaining repetitions under similar conditions.

In most of the observed cases the power and the temperature rise abruptly at the vibration initiation due to the combined high interfacial friction and the viscoelastic power dissipations. Then while the temperature in the weld center increases slowly, the power drops gradually in a transition phase. As soon as the entire weld spot interface reaches the melting temperature of the matrix, the friction heating is eliminated and a sharp strain concentration occurs at those molten interface layers. Due to the quadratic dependency of the consumed power on the strain amplitude, a local intensive volumetric heat is generated. Consequently, the temperature and the power curves undergo a sudden increase. From this point on, the heating is mostly due to viscous vibration dissipation and the temperature continues to rise until around *T=400 °C* and the matrix undergoes a gradual thermal decomposition. During the decomposition a thermal equilibrium occurs at the weld interface where the amount of heat produced by viscous damping and the heat consumed by the decomposition are in balance. This behavior of the temperature and the power curves is typical for this laminate type. However, the onset time for the temperature jump deviates strongly from one weld to another. It can be observed in Fig. 4 that the onset of the second jump of the temperature curve (dashed line) occurs at *t=1.34 s* and reaches the decomposition temperature at *t=1.68 s*. Meanwhile the earliest recorded time for the onset of the temperature jump is *t=0.75 s* and the latest recorded time is *t=2.1 s*. This strong deviation makes it difficult to find an optimum weld duration (t_w) that results a fully diffused weld spot without defects of decomposition.

For the controlled welds C-1 where the power derivative limit is dP_{set}*=100 W/s*, the measured temperature in all of the weld spots remained well below the decomposition temperature. However, the low power derivative limit led in some cases to a rapid reduction of the vibration amplitude and therefore the generated heat energy in the weld spot was insufficient for the matrix to be sustained in the melting temperature zone. As a result most of the weld spots of C-1 were not fully diffused. This can be clearly inferred from the highlighted temperature curve (dashed line) in the plot (Fig. 5 – C-1) which remained almost around *200 °C* and well below the melting temperature of *260 °C*. The problem of the insufficient heat energy is

not present in the C-2 case where the power derivative limit is set at *200 W/s*. In all of the welds performed with this control criteria, the measured temperature exceeded the melting temperature of the matrix. But in some few welds, the temperature in the weld center and for the last *0.5 s* of the weld duration exceeded the decomposition temperature (Fig. 5 – C-2).

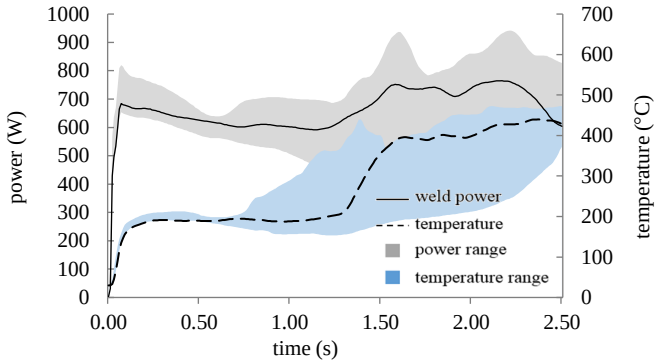

Figure 4 - The time traces of the power and the temperature of the uncontrolled welds (UC-2).

The temperature measurements for the C-3 (dP_{set}=*300 W/s*) show that the welds are exactly in the optimum temperature zone. The temperature of the welds remained almost above the melting and below the decomposition temperatures. The investigations prove that the implemented control method can be useful to eliminate the overheating problem of the weld spots during the differential ultrasonic welding of the composite laminates (Fig. 5 – C-3).

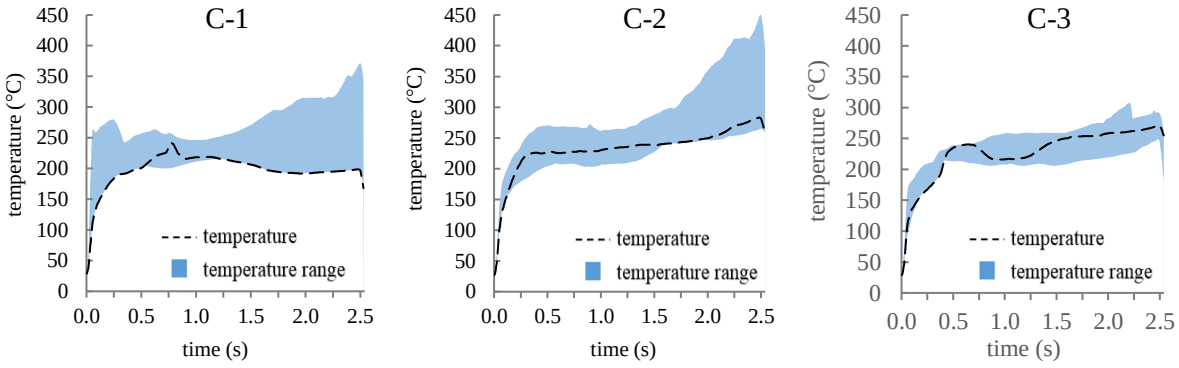

Figure 5. The measured time trace of the temperature in the weld spot for the three controlled weld cases.

4.2. The Weld Strength Analysis

The forces at break resulted from the cross-tension tests are plotted alongside the corresponding weld strengths in Fig. 6. The break force and strength values from the repetitions are averaged and presented as the solid columns; the corresponding standard deviations are plotted as error bars. The lowest break force recorded is for the controlled weld C-1 case at a value of *394 N*, the controlled welds C-2 & C-3 exhibit

almost equal average break forces at *767 N* and *743 N* respectively. On the other hand for the uncontrolled welds it is clearly observed that the break force increases with the increasing weld duration. The maximum average break force of *771 N* is measured for the UC-3 (t_w=*3 s*), which in turn is slightly higher than the controlled weld C-2 case. The ultimate maximum break force throughout the experiments is recorded for the UC-2 case at *892 N* for a weld duration of t_w=*2.5 s*.

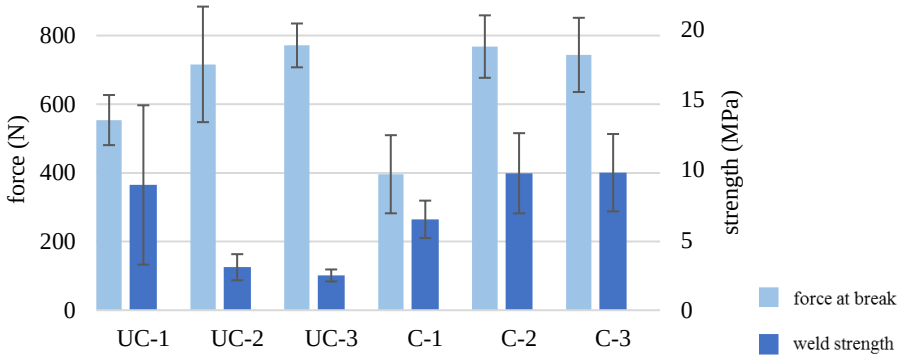

Figure 6. The average force at break and the weld strength in the cross-tension test of the welded samples. (Each corresponding standard deviation is plotted as the error bar above the columns).

The measurements show significant higher weld strength values for the controlled welds than the uncontrolled ones. The average measured weld strengths are plotted as dark blue bars in Fig. 6. The highest weld strengths are measured for the controlled C-2 & C-3 at *9.75 MPa* and *9.8 MPa* respectively. The uncontrolled weld UC-1 is second in rank at *8.9 MPa*. Even though the weld strengths of the controlled welds (C-2 & C-3) are quite close to the uncontrolled UC-1 case. However, the UC-1 weld strength values exhibit extremely large deviations from the average and more importantly it results a much lower average break force in comparison to the C-2 & C-3. The averaged UC-3 weld have the lowest strength (*2.47 MPa*) although it has the highest breaking force. This low weld strengths for UC-2 & UC-3 are caused by the fact that the weld spot overheating creates a large weld spot, but the matrix decomposition in the central area of the spot reduces the quality of the fusion bond and causes joint defects.

5. Conclusions

The influence of the developed logical control system on the weld strength of the differential ultrasonic welded fiber-reinforced thermoplastic laminates was investigated. The mechanical testing was done through the cross-tension test for three uncontrolled weld sets and three controlled weld sets. The uncontrolled welds were investigated for three weld durations. The controlled welds were carried out under a constant weld duration of *2.5 s* but the weld control criteria was varied. The control system checks the power time derivative, if the derivative exceeds a pre-set value then the weld vibration amplitude is stepwise reduced. From the investigations it is found that:

- The power time derivative of the welder is an effective trigger to reduce the amplitude in order to eliminate the overheating problem of the weld spot during the DUS process.
- The controlled welds with a criteria of dP_{set3}=*300 W/s* resulted the highest weld spot strength (*9.8 MPa*) in comparison to the other investigated cases.

- Controlling with small dP_{set} limit values such as *100 W/s*, causes a rapid drop in the ultrasonic amplitude and results in an insufficient heat energy generation for the matrix to reach the melting temperature.
- Even that the uncontrolled welding with a duration of *3 s* resulted in the highest average breaking force of *771 N*, but the weld strength is measured to be the lowest at a value of *2.47 MPa*.
- Most of the controlled weld spots remained below the thermal decomposition temperature of the matrix and above the melting temperature throughout the duration of the ultrasonic welding.

Acknowledgements

Thanks to the BMW Group for supporting this research project and providing the necessary material, equipment and laboratories for the experiments. Special thanks to Robert Carl, Kerem Ucar, Florian Buchner and Albert Fellermayer for their contributions in the research work and their support in conducting the numerous tests and measurements.

References

[1] A. Yousefpour, M. Hojjati, and J.-P. Immarigeon, "Fusion Bonding/Welding of Thermoplastic Composites," *Journal of Thermoplastic Composite Materials*, vol. 17, no. 4, pp. 303–341, 2016.
[2] C. Ageorges, L. Ye, and M. Hou, "Advances in fusion bonding techniques for joining thermoplastic matrix composites: A review," *Composites Part A: Applied Science and Manufacturing*, vol. 32, no. 6, pp. 839–857, 2001.
[3] J. Rotheiser, *Joining of plastics: Handbook for designers and engineers*, 3rd ed. Munich, Cincinnati, Ohio: Hanser Publishers; Hanser Publications, 2009.
[4] A. Benatar and T. G. Gutowski, "Ultrasonic welding of PEEK graphite APC-2 composites," (af), *Polym. Eng. Sci.*, vol. 29, no. 23, pp. 1705–1721, 1989.
[5] A. Benatar, R. V. Eswaran, and S. K. Nayar, "Ultrasonic welding of thermoplastics in the near-field," (en), *Polym. Eng. Sci.*, vol. 29, no. 23, pp. 1689–1698, 1989.
[6] A. Benatar and Z. Cheng, "Ultrasonic welding of thermoplastics in the far-field," (en), *Polym. Eng. Sci.*, vol. 29, no. 23, pp. 1699–1704, 1989.
[7] I. F. Villegas, "In situ monitoring of ultrasonic welding of thermoplastic composites through power and displacement data," (en), *Journal of Thermoplastic Composite Materials*, vol. 28, no. 1, pp. 66–85, 2014.
[8] A. Levy, S. Le Corre, and I. Fernandez Villegas, "Modeling of the heating phenomena in ultrasonic welding of thermoplastic composites with flat energy directors," (en), *Journal of Materials Processing Technology*, vol. 214, no. 7, pp. 1361–1371, 2014.
[9] Tian Zhao, Genevieve Palardy, Irene Fernandez Villegas, Calvin Rans, and Rinze Benedictus, *Comparative analysis of in-plane and out-of-plane mechanical behavior of spot-welded and mechanically fastened joints in thermoplastic composites: 17th European Conference on Composite Materials, Munich, Germany, 26 - 30th June 2016*.
[10] D. A. Grewell, "Simultaneous amplitude and force profiling during ultrasonic welding of thermoplastic workpieces," US 5855706 A.